Monovalent and Divalent Cation Permeability and Block of Neuronal Nicotinic Receptor Channels in Rat Parasympathetic Ganglia

THOMAS J. NUTTER and DAVID J. ADAMS

From the Department of Molecular and Cellular Pharmacology, University of Miami School of Medicine, Miami, Florida 33101

ABSTRACT   Acetylcholine-evoked currents mediated by activation of nicotinic receptors in rat parasympathetic neurons were examined using whole-cell voltage clamp. The relative permeability of the neuronal nicotinic acetylcholine (nACh) receptor channel to monovalent and divalent inorganic and organic cations was determined from reversal potential measurements. The channel exhibited weak selectivity among the alkali metals with a selectivity sequence of $Cs^+ > K^+ > Rb^+ > Na^+ > Li^+$, and permeability ratios relative to Na^+ (P_x/P_{Na}) ranging from 1.27 to 0.75. The selectivity of the alkaline earths was also weak, with the sequence of $Mg^{2+} > Sr^{2+} > Ba^{2+} > Ca^{2+}$, and relative permeabilities of 1.10 to 0.65. The relative Ca^{2+} permeability (P_{Ca}/P_{Na}) of the neuronal nACh receptor channel is ~ fivefold higher than that of the motor endplate channel (Adams, D. J., T. M. Dwyer, and B. Hille. 1980. *Journal of General Physiology*. 75:493–510). The transition metal cation, Mn^{2+} was permeant (P_x/P_{Na} = 0.67), whereas Ni^{2+}, Zn^{2+}, and Cd^{2+} blocked ACh-evoked currents with half-maximal inhibition (IC_{50}) occurring at ~500 μM, 5 μM and 1 mM, respectively. In contrast to the muscle endplate AChR channel, that at least 56 organic cations which are permeable to (Dwyer et al., 1980), the majority of organic cations tested were found to completely inhibit ACh-evoked currents in rat parasympathetic neurons. Concentration-response curves for guanidinium, ethylammonium, diethanolammonium and arginine inhibition of ACh-evoked currents yielded IC_{50}'s of ~2.5–6.0 mM. The organic cations, hydrazinium, methylammonium, ethanolammonium and Tris, were measureably permeant, and permeability ratios varied inversely with the molecular size of the cation. Modeling suggests that the pore has a minimum diameter of 7.6 Å. Thus, there are substantial differences in ion permeation and block between the nACh receptor channels of mammalian parasympathetic neurons and amphibian skeletal muscle which represent functional consequences of differences in the primary structure of the subunits of the ACh receptor channel.

INTRODUCTION

Neuronal nicotinic acetylcholine receptor (nAChR) channels are distributed throughout the central and peripheral nervous systems, and are structurally, pharmacologically and functionally distinct from the nAChR channel at the motor endplate. Whereas the muscle-type nAChR is a pentameric structure composed of two ACh-binding subunits ($\alpha 1$) and three structural subunits ($\beta 1$, δ, γ, or ϵ), the neuronal nAChR appears to be comprised of two types of subunit, the α-subunit and the β (or non-α) subunit. The stoichiometry for the neuronal nAChR expressed in *Xenopus* oocytes has been defined as 2α, 3β (Anand, Conroy, Schoepfer, Whiting, and Lindstrom, 1991; Cooper, Couturier, and Ballivet, 1991), however, it remains to be confirmed in neurons. At present, seven functional α-subunits ($\alpha 2$, $\alpha 3$, $\alpha 4$, $\alpha 5$, $\alpha 7$, $\alpha 8$, and $\alpha 9$) and two functional β-subunits ($\beta 2$, $\beta 4$) have been identified (see reviews by Papke, 1993; Sargent, 1993). Muscle nAChRs differ from neuronal nAChRs in their pharmacological sensitivity to receptor antagonists, for example, the specificity of antagonism by α-bungarotoxin and neuronal-bungarotoxin for nAChRs in skeletal muscle and neurons, respectively (for review see Lukas and Bencherif, 1992). Differences in agonist potency and block by neurotoxins have also been reported among neuronal nAChRs composed of different subunit combinations (Leutje, Wada, Rogers, Abramson, Tsui, Heinemann, and Patrick, 1990; Luetje and Patrick, 1991). It would appear that nAChRs are a heterogeneous family of neurotransmitter-activated channels with a diverse range of functional properties.

The permeability and conductance properties of the muscle-type nAChR channel have been studied extensively (Adams, Dwyer, and Hille, 1980; Adams, Nonner, Dwyer, and Hille, 1981; Dani and Eisenman, 1987; Decker and Dani, 1990; Lewis, 1979, 1984), whereas the functional properties of neuronal nAChRs are less clearly defined. The Ca^{2+} permeability of the neuronal nAChR channel has been examined in PC12 cells (Sands and Barish, 1991), bovine chromaffin cells (Vernino, Amador, Luetje, Patrick, and Dani, 1992), rat medial habenula (Mulle, Choquet, Korn, and Changeux, 1992), superior cervical ganglion (Trouslard, Marsh, and Brown, 1993) and parasympathetic intracardiac neurons (Fieber and Adams, 1991; Adams and Nutter, 1992). The monovalent cation permeability of the nAChR channel in bovine chromaffin cells was also examined (Nooney, Peters, and Lambert, 1992), but this study was limited to alkali metal cations, as was a study of the unitary conductance properties of the nAChR channel in rat sympathetic neurons (Mathie, Cull-Candy, and Colquhoun, 1991). No extensive quantitation of the ionic selectivity or permeability properties of neuronal nAChR channels has been undertaken.

Ionic currents evoked by ACh in rat intracardiac neurons are mimicked by brief pulses of nicotine to the neuronal soma, are insensitive to atropine, and are inhibited by the ganglionic nicotinic antagonists mecamylamine, hexamethonium and neuronal bungarotoxin (Fieber and Adams, 1991), consistent with the activation of nicotinic AChR channels. In this study, we examine the permeability of the neuronal nAChR channel of parasympathetic neurons from rat intracardiac ganglia to inorganic and organic cations. The neuronal nAChR channel is weakly selective to monovalent and divalent inorganic cations, and permeable to at least six organic cations. The transition metal cations and many organic cations inhibit currents

through the neuronal nAChR-channel. A preliminary report of some of these results has been presented to the Biophysical Society (Nutter and Adams, 1991).

METHODS

Preparation and Solutions

Parasympathetic neurons from rat atria were isolated and cultured as previously described (Fieber and Adams, 1991). Briefly, atria were dissected from neonatal (1–5 d postpartum) rat and incubated in Krebs solution containing 1 mg/ml collagenase (Worthington-Biomedical Corp., Freehold, NJ) for 1 h at 37°C. Intracardiac ganglia were dissected from the atria and transferred to a sterile culture dish containing culture medium (Dulbecco's Modified Eagle Medium with 10 mM glucose, 10% (vol/vol) fetal calf serum, 100 U/ml penicillin, and 0.1 mg/ml streptomycin), triturated with a fine bore pasteur pipette, then plated onto 18-mm glass coverslips coated with laminin. The dissociated cells were incubated at 37°C under a 95% air, 5% CO_2 atmosphere. Electrophysiological recordings were made from neurons maintained in tissue culture for 36–72 h. At the time of experiments, the glass coverslip was transferred to a low volume (0.5 ml) recording chamber and viewed at 400× magnification using an inverted, phase contrast microscope. Experiments were conducted at room temperature (21–23°C).

The extracellular reference solution (physiological salt solution, PSS) consisted of (in millimolar): 140 NaCl, 1 $CaCl_2$, 7.7 glucose, 10 histidine, pH 7.2. The relative permeability of the ACh-activated channel to inorganic and organic cations was investigated by replacement of NaCl with an osmotically equivalent amount of the chloride salt of the test cation. Inorganic salts replacing NaCl in test solutions include LiCl, KCl, RbCl, CsCl, NH_4Cl, $MgCl_2$, $CaCl_2$, $SrCl_2$, $BaCl_2$, and $MnCl_2$, all of analytical grade. The test solutions for divalent cations contained 100 mM of the chloride salt, and all solutions had a pH of 7.2. The following organic compounds were substituted for NaCl in the test solutions: formamidine.HCl, methylamine-.HCl, ethylamine.HCl, dimethylamine.HCl, acetamidine.HCl, methylethanolamine.HCl, etha-nolamine.HCl, diethanolamine.HCl, arginine.HCl, 1,3-Bis[tris(hydroxymethyl)-methylamino]-propane (Bis-Tris), glucosamine.HCl (all from Aldrich Chemical Company, Milwaukee, WI), tris(hydroxymethyl)aminomethane.HCl (Tris), lysine.HCl, glycine methyl ester.HCl (all from Sigma Chemical Company, St. Louis, MO), hydrazine and guanidine.HCl (Eastman Kodak Company, Rochester, NY). When the test cation source compound was a free amine, it was titrated with HCl to the desired pH. All organic solutions had a pH of 7.2, with the exceptions of hydrazine.Cl (pH 6.6), glycine methylester (pH 5.9), Tris (pH 6.8), and glucosamine (pH 6.3), which were studied at a slightly more acidic pH to increase the ionized concentration of the test ion. Bis-Tris was studied at pH 8.0 at which the molecule is predominantly in the monovalent cationic form. For some organic test solutions it was necessary to use mixtures of 50% Na^+/50% organic cation in order to obtain clearly discernable currents. In these experiments, measurements of reversal potential shifts were made in relation to the external reference solution (140 mM NaCl), and compared to a solution in which 50% of the NaCl was replaced with an osmotically equivalent concentration of mannitol (140 mM). Mannitol was chosen over salts of large positively charged ions, such as N-methylglucamine, because the amplitude of the ACh-evoked current in the presence of N-methylglucamine was less than predicted for the extracellular Na^+ concentration ($[Na^+]_o$) (see Adams et al., 1981; Sanchez, Dani, Siemen, and Hille, 1986). In the text, the neutral basic or charged ionic name of the organic cations are used interchangeably. Reversal potential measurements were corrected for differences in junction potential between the bath solution and the indifferent electrode (0.15 M KCl/agar bridge). Liquid junction potential measurements to the indifferent electrode were made with respect to a reference electrode (saturated KCl, reverse sleeve junction; Corning

X-EL 47619). The osmotic pressure of the solutions was monitored with a vapor pressure osmometer (Wescor 5500).

The intracellular pipette solution contained (in millimolar): 130 NaCl, 2 Na$_2$ATP, 5 Na$_4$BAPTA, 10 N-2-hydroxy-ethylpiperazine-N'-2-ethansulfonic acid (HEPES)-NaOH, pH 7.2. ACh-evoked currents were investigated in response to pressure application (Picospritzer II, General Valve Corp., Fairfield, NJ) of 100 μM AChCl, added to the appropriate test solution, from an extracellular micropipette. The pressure ejection pipette was positioned ~50 μm from the soma membrane to evoke maximal responses to agonist under control conditions (10 ms, 10 psi). To minimize receptor desensitization, a delay of >60 s between agonist applications was maintained. Agonist was applied during continuous bath perfusion at a rate of ~2 ml/min. To ensure total exchange of the external reference and test solutions during the course of an experiment, the recording chamber was perfused with a minimum of 20 vol (10 ml) of solution.

Current Recording

Agonist-induced responses of cultured intracardiac neurons were studied under voltage clamp using the whole-cell recording configuration of the patch clamp technique (Hamill, Marty, Neher, Sakmann, and Sigworth, 1981). Membrane current was monitored using a patch clamp amplifier (L/M EPC-7, List Electronic, Darmstadt, Germany), filtered at 10 kHz (−3 dB) with a low pass, 4-pole Bessel filter and recorded on video tape using an analogue to digital recorder adaptor (PCM-1; Medical Systems, Greenvale, NY). The membrane current was monitored continuously on a digital oscilloscope. The cell capacitance (C_m) was determined for each cell from the compensation of the capacity transient in response to a −10 mV voltage step. No compensation of the series resistance (R_s) was made. However, given that R_s was usually <6 MΩ and the maximum amplitude of whole-cell ACh–evoked currents near the reversal potential was <50 pA, then the voltage error due to R_s would be <0.3 mV. Whole-cell currents were displayed using a chart recorder and individual current traces were recorded on disc using the Axotape program (Axon Instruments, Inc., Foster City, CA) for subsequent analysis.

Data Analysis

The reversal (zero-current) potential, E_{rev}, for ACh-activated currents in the various test solutions was determined from peak current amplitude evoked in response to ACh during steps to different membrane potentials in 5-mV increments straddling E_{rev}. Responses obtained in test solutions were preceded and followed by recordings in the reference solution. Pronounced inward rectification of the ACh-evoked currents required measurements of ΔE_{rev} to be based on clearly defined ACh-evoked inward and outward currents recorded around the reversal potential. Test measurements were rejected if E_{rev} in the reference solution changed by 3 mV or more, or if distinct inward and outward currents could not be resolved. Peak current values were measured by cursor using the Axotape program. Reversal potentials were determined by interpolation of polynomial fits of at least six peak current values obtained at membrane potentials on either side of E_{rev}. Relative permeability estimates for cations were calculated using the Goldman-Hodgkin-Katz (GHK) voltage equation (see Hille, 1975). The form of the equation used to determine the relative permeabilities from shifts in reversal potential (ΔE_{rev}) was;

$$\frac{P_X}{P_{Na}} = \exp \Delta E_{rev}\, F/RT \cdot \frac{[Na^+]_i}{[X^+]_o} \tag{1}$$

where RT/F is 25.4 mV at 22°C, P_X/P_{Na} is the permeability ratio for X^+, and $[Na^+]_i$ and $[X^+]_o$ are the ion concentrations of the internal and external solutions, respectively. To determine the relative permeability to divalent cations, the GHK equation was modified to include divalent

cations and activity coefficients (Lewis, 1979; Fieber and Adams, 1991). Activity coefficients of the salts were obtained from Butler (1968) and Robinson and Stokes (1965).

The reduction of the ACh-evoked current amplitude by external cations was determined by measuring the peak amplitude in the presence of the test (blocking) cation (I) which was normalized to that obtained in the absence of the test cation (I_{max}). Dose-response data were fitted with a single site adsorption isotherm according to the following equation:

$$\frac{I}{I_{max}} = \frac{1}{1 + \left(\frac{IC_{50}}{[X]}\right)} \tag{2}$$

where I/I_{max} is the relative current amplitude, X is the test cation concentration, and IC_{50} is the cation concentration that produces 50% inhibition of the maximum response. All numerical data are presented as mean $\pm$ SEM, with the number of experiments in parentheses.

RESULTS

ACh-induced Current-Voltage Relationship

Application of a brief pulse of ACh (100 μM) from a pressure ejection pipette to a voltage-clamped parasympathetic neuron evoked a transient inward current at negative membrane potentials, with the amplitude dependent on the membrane potential (Fig. 1 A). The average amplitude of the ACh-induced currents in six cells at -90 mV was -446 ± 137 pA, and normalized to the cell capacitance of 15 ± 1 pF ($n = 6$), the current density was ~ 30 pA/pF. The response of the same cell to exogenous application of 100 μM nicotine is shown in Fig. 1 B. Currents evoked by nicotine were typically smaller than those elicited by similar concentrations of ACh, with a mean amplitude of -198 ± 74 pA at -90 mV, corresponding to an average current density of 14 pA/pF. The current-voltage (I-V) relationships for ACh- and nicotine-induced responses obtained in PSS are shown in Fig. 1 C. The reversal (zero-current) potential for ACh-mediated currents in near symmetric Na^+ solutions averaged $+3.4 \pm 1.4$ mV ($n = 6$), and currents elicited by nicotine exhibited no significant difference in reversal potential ($+4.3 \pm 2.2$ mV, $n = 6$). The whole-cell currents evoked by ACh and nicotine exhibited a marked rectification, with larger responses obtained at negative membrane potentials than at the corresponding positive potentials. Inward rectification was observed in the absence of divalent cations in either the intra- or extracellular solution, suggesting that the reduction in outward current at positive membrane potentials is unlikely to be due to divalent cation (Mg^{2+}) block of the ion channel (Fieber and Adams, 1991).

Inorganic Cation Selectivity of the Neuronal ACh Receptor Channel

The neuronal nAChR channel of rat parasympathetic neurons exhibits weak selectivity among the monovalent alkali metals. Superimposed current traces recorded at 5-mV intervals around the reversal potential obtained in PSS and after substitution of various monovalent test cations for Na^+ in the external solution are shown in Fig. 2 A. Shifts in reversal potential, ΔE_{rev}, were determined from plots of peak current amplitude versus membrane potential in test solutions relative to that obtained in the Na^+ reference solution. The average I-V relationships obtained for K^+, NH_4^+, and Li^+

THE JOURNAL OF GENERAL PHYSIOLOGY · VOLUME 105 · 1995

in reference to Na^+ are shown in Fig. 2 B. The observed shifts in E_{rev} for the alkali metals, as well as their permeabilities relative to Na^+ (P_x/P_{Na}), calculated according to Eq. 1, are listed in Table I. The selectivity sequence of the neuronal nAChR channel for monovalent cations follows the order; $NH_4^+ > Cs^+ > K^+ > Rb^+ > Na^+ > Li^+$, with permeability ratios of 2.09, 1.27, 1.23, 1.11, 1.00, and 0.75, respectively.

The neuronal nicotinic AChR channel was also permeable to the divalent alkaline earths and the transition metal cation, Mn^{2+}. ACh-evoked currents obtained after
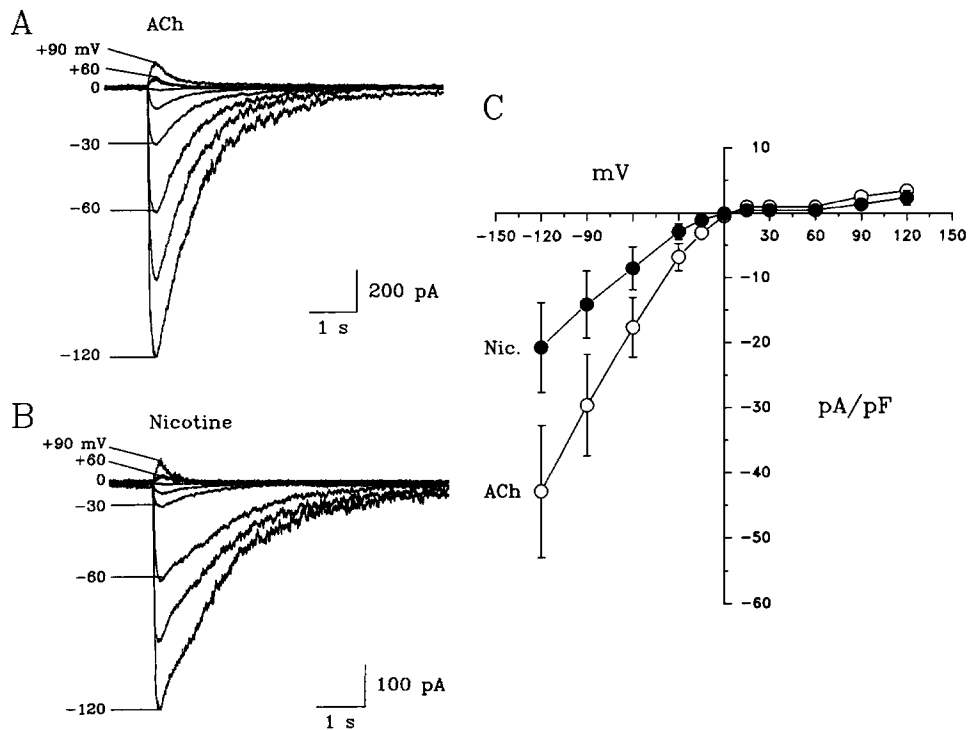

FIGURE 1. Excitatory ACh-evoked currents in isolated parasympathetic neurons dissociated from rat intracardiac ganglia. (A) Whole-cell currents evoked in response to a 10-ms pulse of 100 μM ACh applied from an extracellular pipette, at the membrane potentials indicated. (B) Whole-cell currents elicited in response to a 10-ms pulse of 100 μM nicotine from an extracellular pipette. Same cell as in A. (C) Current-voltage (I-V) relationship for peak current amplitude evoked by ACh (O) and nicotine (●) in external Na^+ solution. Each point represents the mean current density (pA/pF) ± SEM from six cells.

isoosmotic substitution of Ca^{2+}, Mg^{2+}, Sr^{2+}, or Ba^{2+} for Na^+ are shown in Fig. 3 A. A substantial inward current was observed after replacement of Na^+ with osmotically equivalent concentrations of divalent test cations indicating that the neuronal nAChR channel is permeable to divalent cations. The peak ACh-evoked conductance obtained in the presence of isotonic Ca^{2+} was ~65% of that obtained in isotonic (140 mM) Na^+. The I-V relationships for the alkaline earth cations are shown in Fig. 3 B. Substitution of the divalent cations for Na^+ shifted E_{rev} to more negative values and reduced peak current amplitude (Fig. 2 B). The shifts in reversal potential and
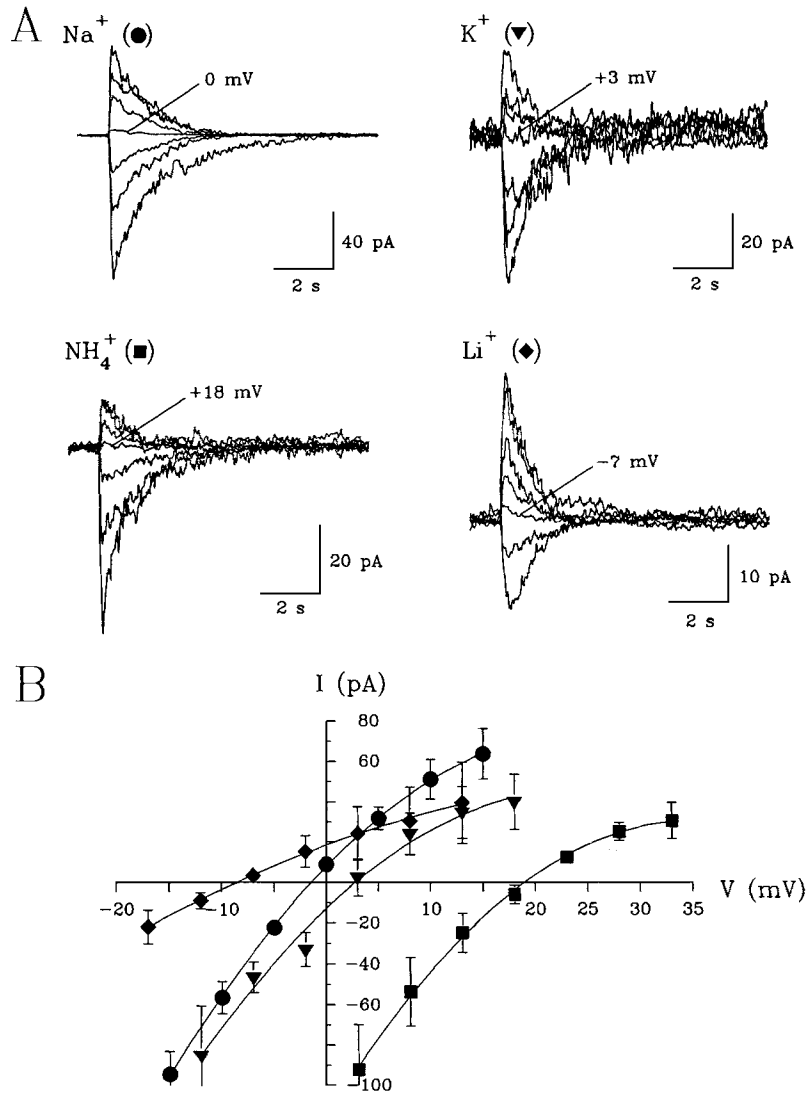
FIGURE 2. Reversal potential measurements of ACh-evoked currents obtained in the presence of monovalent inorganic cations. (A) Whole-cell ACh-evoked currents obtained at 5-mV increments around the reversal potential in an extracellular Na^+ (●) solution, and after isoosmotic replacement of Na^+ with K^+ (▼), NH_4^+ (■) or Li^+ (◆). (B) I-V relations in the reference Na^+ solution, and in isotonic K^+, Li^+, and NH_4^+ test solutions. The reversal potential shifted from -1.9 mV in the Na^+ reference solution, to -9.2 mV in Li^+, $+3.4$ mV in K^+, and $+18.1$ mV in NH_4^+ test solutions. Symbols same as in A. Each point represents the mean peak current amplitude ± SEM of at least four cells.

corresponding relative permeabilities for the divalent metals are summarized in Table II. Mg^{2+} produced the smallest shift in E_{rev} (-1.6 ± 0.6 mV, $n = 4$), and was the only divalent cation with a permeability greater than Na^+ ($P_{Mg}/P_{Na} = 1.1$). The selectivity sequence for the divalent cations was $Mg^{2+} > Sr^{2+} > Ba^{2+} > Mn^{2+} \geq$

Ca^{2+}, with permeability ratios of 1.10, 0.78, 0.72, 0.67, and 0.65, respectively. The selectivity sequence for the alkaline earths correlates inversely with the hydrated radii of these divalent cations.

In experiments to examine the relative permeabilities of the transition metal cations Ni^{2+}, Zn^{2+}, and Cd^{2+}, ACh-evoked currents could be detected in neither isotonic solutions nor 50% Na^+ mixtures of these cations. In fact, low concentrations of these transition metal divalent cations inhibited ACh-induced currents. ACh-evoked currents obtained in the presence of extracellular Na^+ solutions containing 0, 3 μM and 30 μM Zn^{2+} are shown in Fig. 4 A. The reduction in ACh-induced peak current amplitude with increasing concentrations of external Zn^{2+} was fitted by a single-site adsorption isotherm yielding half-maximal current inhibition (IC_{50}) of 5.2 μM Zn^{2+}. Average I-V relationships determined in the absence and presence of 10 μM Zn^{2+} for four neurons are shown in Fig. 4 B. The inhibition of the ACh-evoked current by Zn^{2+} was increased by membrane hyperpolarization. A linearized plot of the ratio of the control ACh-evoked current amplitude to that obtained in the presence of 10 μM Zn^{2+} (Λ-1) as a function of the membrane potential (Fig. 4 C)

TABLE I

ΔE_r and Relative Permeabilities for Monovalent Cations

X		$\Delta E_r \pm$ SEM		P_X/P_{Na}
	mM	mV	n	
NH_4^+	140	$+20.0 \pm 1.2$	5	2.09
Cs^+	140	$+6.0 \pm 0.3$	4	1.27
K^+	140	$+5.3 \pm 0.5$	4	1.23
Rb^+	140	$+2.7 \pm 1.0$	5	1.11
Na^+	140	0.0	—	1.00
Li^+	140	-7.3 ± 0.5	4	0.75

External reference solution (in millimolar): 140 NaCl, 7.7 Glucose, 10 Histidine, pH 7.2. Internal solution (in millimolar): 130 NaCl, 2 Na_2ATP, 5 Na_4BAPTA, 10 HEPES, pH 7.2.

revealed an e-fold change per -188 mV change in the membrane potential. This voltage sensitivity of the block of neuronal nAChR channels by Zn^{2+} is equivalent to that of a binding site $\sim 7\%$ into the membrane field of the channel protein (Woodhull, 1973). Dose-response curves determined for inhibition of ACh-evoked currents by Ni^{2+} and Cd^{2+} indicate that at a membrane potential of -90 mV, ~ 500 μM Ni^{2+}, and ~ 1 mM Cd^{2+} block one half of the conductance. The block of ACh-evoked currents produced by all of these transition metal cations was cumulative with repeated ACh application and recovery was incomplete after >30 min washout.

pH Dependence of ACh-evoked Currents

The effect of external pH on ACh-evoked current amplitude and reversal potential was examined, a necessary control experiment given that the pK_a of several organic compounds is <9.0. The relative permeability of these cations was examined at pH <7 in order that the test cation was predominantly in the ionized form. Histidine base (pK_a's = 1.8, 6.0, and 9.2) was chosen as the buffer and the reference solution (PSS) was titrated to the test pH (pH 5.0–9.0) with HCl. ACh-induced currents
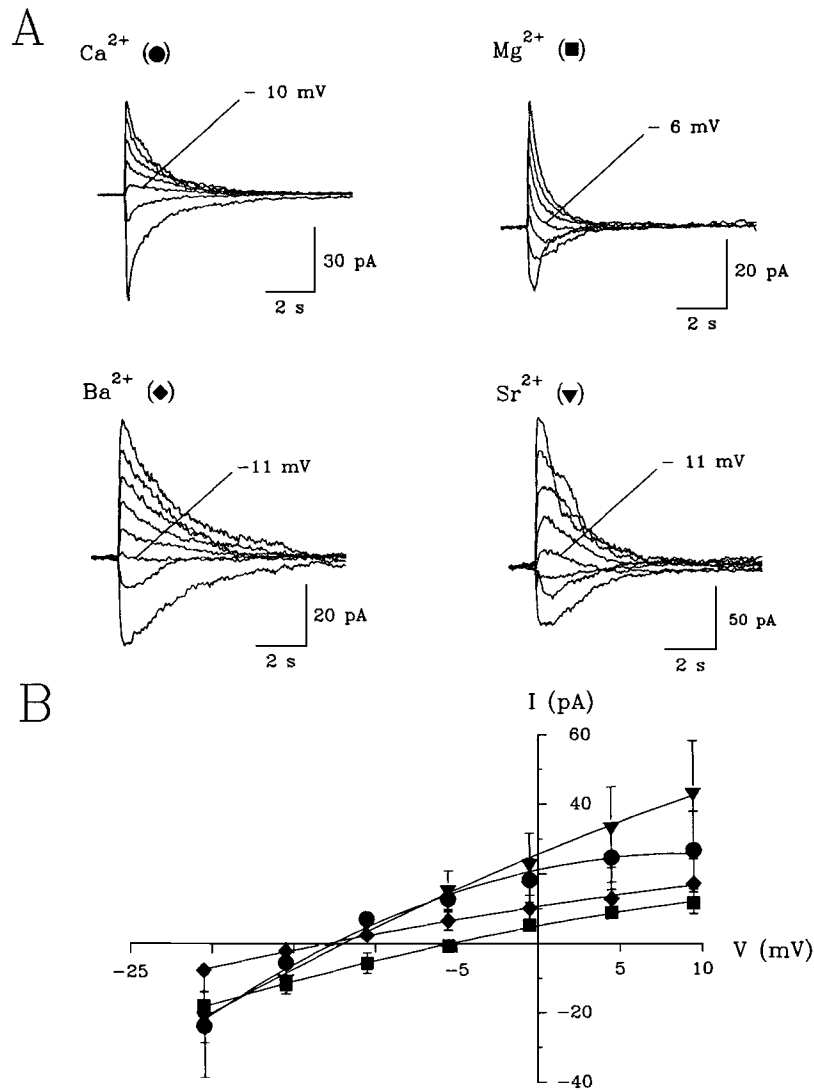
FIGURE 3. Reversal potential measurements of ACh-evoked currents obtained in the presence of alkaline earth divalent cations. (A) Whole-cell currents recorded in the presence of 100 mM Ca^{2+} (●), Mg^{2+} (■), Ba^{2+} (◆), and Sr^{2+} (▼) in response to a 10-ms pulse of ACh at membrane potentials from -20 to $+10$ mV in 5-mV increments. (B) I-V relations for isotonic Ca^{2+}, Mg^{2+}, Ba^{2+} and Sr^{2+}. Substitution of divalent metal cations for Na^+ in the external solution reduced the ACh-evoked inward current amplitude and shifted the reversal potential to more negative membrane potentials. Symbols same as in A. Each point represents the mean peak current amplitude ± SEM of at least four cells.

recorded in the same cell at pH 7.0, 8.0, and 9.0 are illustrated in Fig. 5 A. ACh-evoked peak current amplitude was maximal at pH 8.0 and was reduced at both more acidic and basic pH. Whereas the current amplitude was maximal at pH 8.0, the reversal potential did not change with external pH (Fig. 5 B). pH changes

affected both inward and outward current amplitudes. Relative peak current amplitudes measured at membrane potentials of -15 and $+15$ mV are plotted versus external pH in Fig. 5 C ($n = 3$). The reduction in current amplitude was independent of membrane potential. No ACh-evoked currents were detected at a pH ≤ 5.0. These results suggest that channel conductance depends on a titratable ionic group with a pK_a of ~ 6.7, situated outside the membrane electric field. Another series of experiments conducted with morpholinopropanesulfonic acid (MOPS) as the buffer yielded a pK_a of 6.8, indicating that protonation of the extracellular histidine buffer is unlikely to be responsible for the block of ACh-mediated currents.

Organic Cation Permeation in the Neuronal nAChR Channel

The permeability of the neuronal nAChR-channel to organic cations of varied molecular dimensions was assessed by reversal potential shifts relative to Na^+. Superimposed ACh-evoked current traces obtained at membrane potentials around the reversal potential, and after replacement of Na^+ with monovalent organic cations are shown in Fig. 6 A. The I-V relationships for hydrazine (pH 6.6), methylamine and

TABLE II

ΔE_r and Relative Permeabilities for Divalent Cations

X	$\Delta E_r \pm$ SEM			P_X/P_{Na}
	mM	mV	n	
Mg^{2+}	100	-1.6 ± 0.6	4	1.10
Sr^{2+}	100	-8.1 ± 0.7	4	0.78
Ba^{2+}	100	-9.7 ± 0.9	5	0.72
Mn^{2+}	100	-10.7 ± 1.2	4	0.67
Ca^{2+}	100	-11.0 ± 0.1	5	0.65

External reference solution (in millimolar): 140 NaCl, 7.7 Glucose, 10 Histidine, pH 7.2. Internal solution (in millimolar): 130 NaCl, 2 Na_2ATP, 5 Na_4BAPTA, 10 HEPES, pH 7.2.

ethanolamine in relation to Na^+ are plotted in Fig. 6 B. A positive shift in reversal potential was observed in the presence of hydrazine and methylamine, indicating a higher permeability than Na^+, whereas a shift of E_{rev} in the negative direction indicated that ethanolamine was less permeant. In contrast to the observed increases of ACh-evoked current amplitude at the frog motor endplate (Dwyer et al., 1980), hydrazine and methylamine produced a significant decrease in the peak current amplitude of the neuronal ACh-evoked currents. The abilities of the following ammonium and guanidinium derivatives to carry inward current were also tested: formamidine, ethylamine, dimethylamine, acetamidine, guanidine, methylethanolamine, glycine methylester, diethanolamine and arginine. Application of exogenous ACh in isotonic (140 mM) solutions of these test cations elicit neither inward nor outward currents.

In an attempt to prevent channel block due to isotonic concentrations of these cations, mixtures of 50% Na^+/50% organic cation were tested. Shifts in reversal potential for such mixtures were determined with respect to the reference solution (140 mM NaCl). ACh-evoked currents obtained in 50% Na^+/50% mannitol exhibited
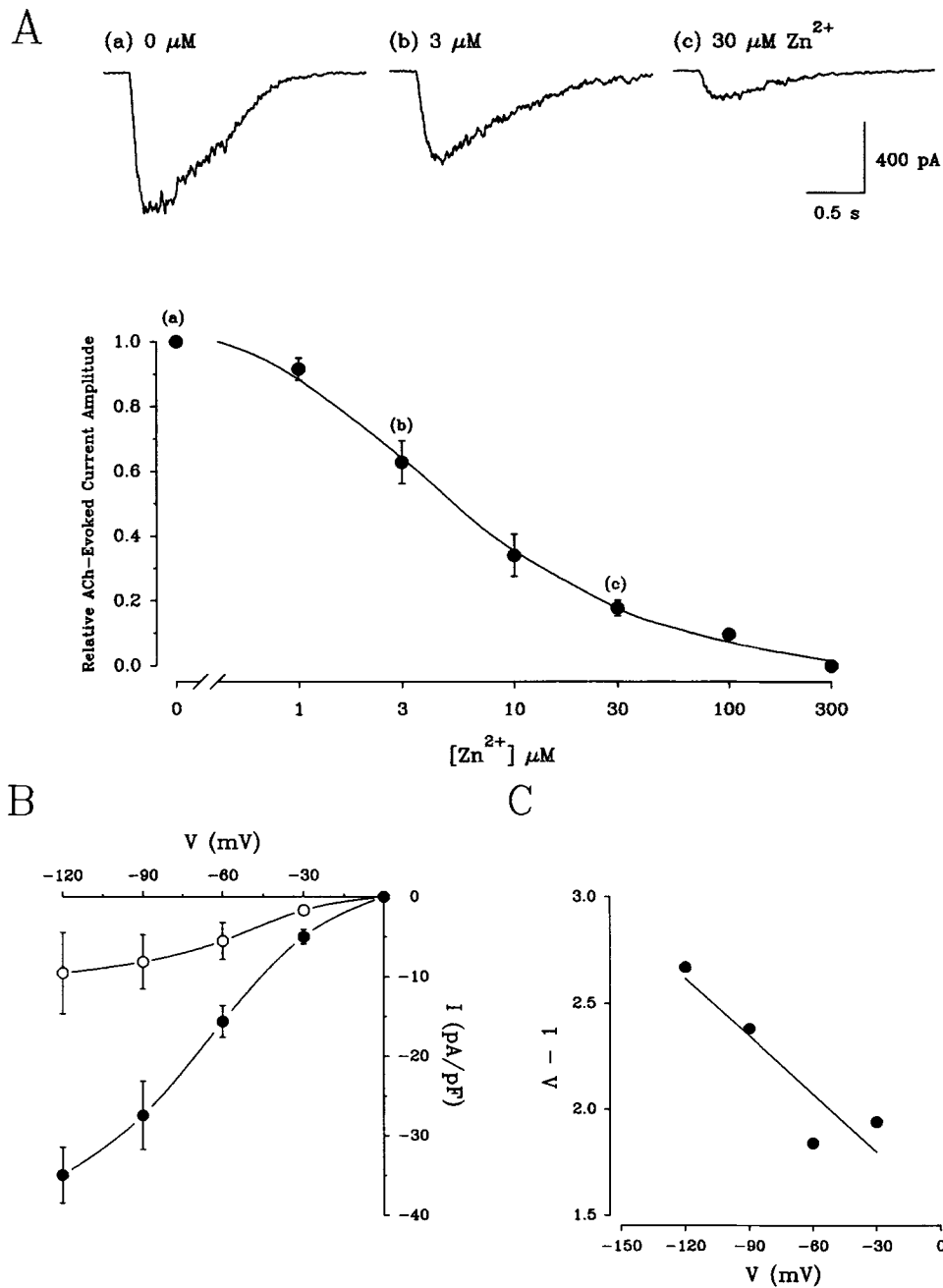
FIGURE 4. Inhibition of ACh-evoked currents by external zinc ions. (A) Relative whole-cell ACh-evoked current amplitude plotted as a function of the external Zn^{2+} concentration. Zn^{2+} was added to the extracellular Na^+ solution at the concentrations indicated and the ACh-evoked current amplitude was measured at a holding potential of -90 mV. The curve is a best fit of the data by a single-site adsorption isotherm using Eq. 2 with a half-maximal inhibition (IC_{50}) of ~5 μM. Each data point represents the mean ± SEM for five cells. Representative ACh-induced currents obtained in the absence (a) and presence of 3 μM (b) and 30 μM (c) Zn^{2+} are shown above. (B) I-V relationship of ACh-evoked currents obtained in the absence (●) and presence (○) of 10 μM Zn^{2+}. Each point represents the mean current density ± SEM from four cells. (C) The voltage dependence of Zn^{2+} inhibition of ACh-activated currents. The ratio of current amplitudes (Λ) obtained in the absence and presence of 10 μM Zn^{2+} was determined at different membrane potentials. Λ-1 is plotted as a function of membrane potential. Data points were fitted by linear regression.

a reversal potential of -20.9 ± 0.9 mV ($n = 10$), close to that predicted (-20 mV) by the Nernst equation for a Na^+-selective electrode. With organic cations present in test solutions, E_{rev} would shift to more positive potentials than that obtained with mannitol if the organic cation was permeant. ACh-evoked currents obtained with mixtures of Na^+/mannitol, Na^+/Tris and Na^+/lysine are shown in Fig. 7 A. Although substitution of Tris.Cl or lysine.Cl for mannitol in the test solutions produced a >
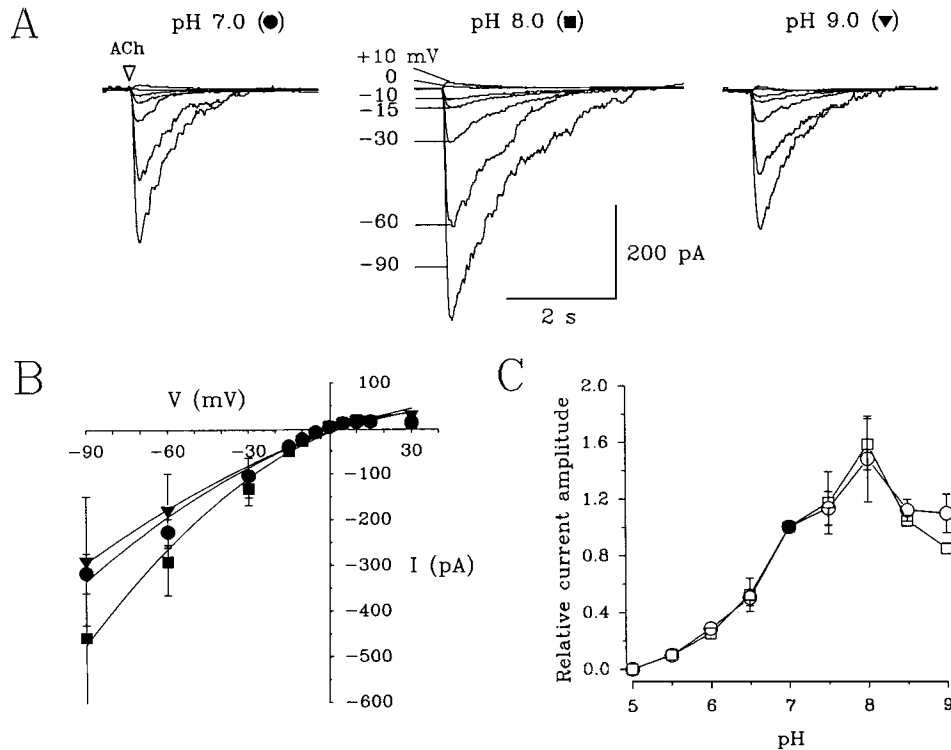
FIGURE 5.   Effect of external pH on ACh-evoked currents. (A) Representative ACh-induced currents obtained from the same cell at pH 7.0 (●), 8.0 (■) and 9.0 (▼). ACh (100 μM, 10 ms) was applied at the holding potentials indicated for the currents shown at pH 8.0. (B) Peak ACh-activated current amplitude plotted as a function of membrane potential at pH 7.0, 8.0, and 9.0. Symbols same as in A. Each data point represents the mean $\pm$ SEM of at least three cells. (C) Relative peak ACh-evoked current amplitude plotted as a function of the external pH. Currents, measured at holding potentials of -15 mV (○) and $+15$ mV (□), were normalized with respect to those obtained at pH 7.0 (filled symbols). Each point represents the mean $\pm$ SEM for at least three cells.

threefold reduction in current amplitude, both inward and outward currents were clearly detectable. The I-V relationships obtained for the 50% Na^+/Tris and 50% Na^+/lysine mixtures exhibited a slight positive shift of E_{rev} relative to that obtained in 50% Na^+/mannitol (Fig. 7 B). No inward or outward currents were evoked by ACh application in 50% mixtures of Na^+ with ethylamine, acetamidine, guanidine, methylethanolamine, glycine methylester, diethanolamine, arginine, glucosamine, or
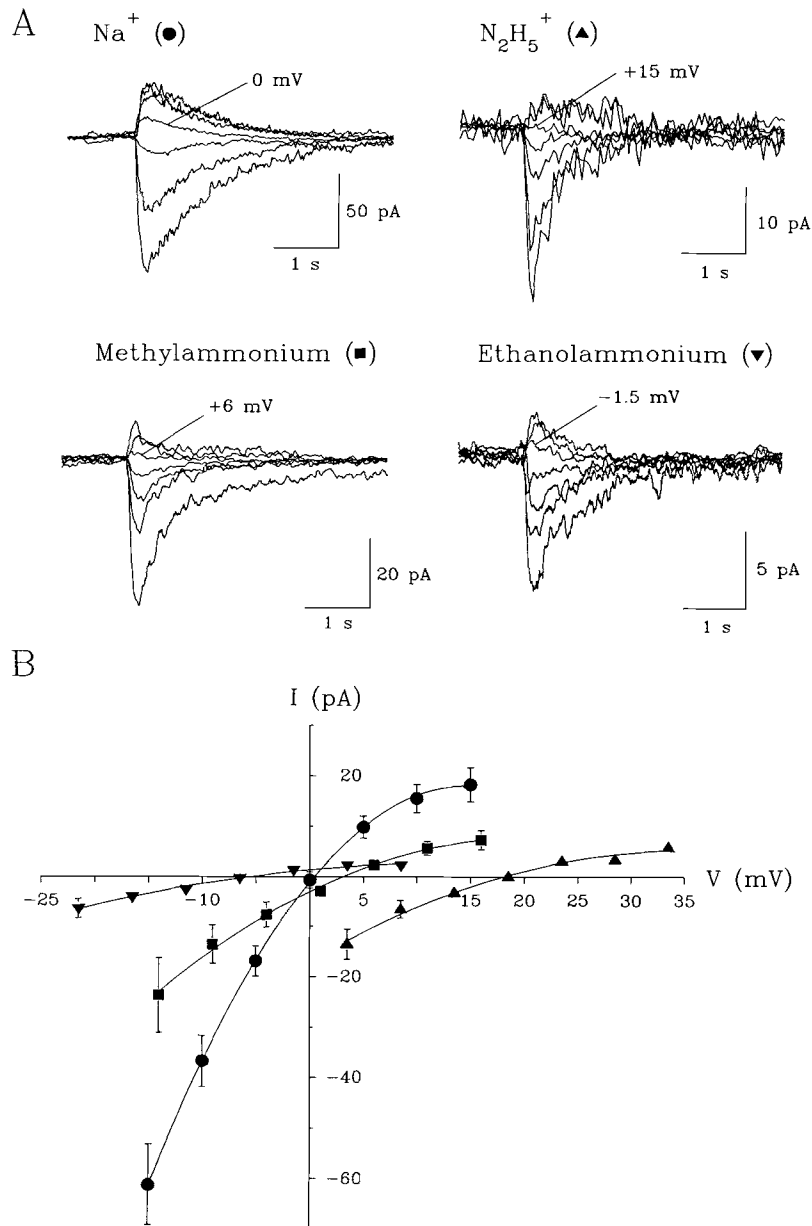
FIGURE 6. Reversal potential measurements of ACh-evoked currents obtained after replacement of extracellular Na^+ with the monovalent organic cations, hydrazinium, methylammonium and ethanolammonium. (*A*) Whole-cell currents elicited at 5-mV intervals by a brief pulse of ACh in the presence of 140 mM Na^+ (●), and after isoosmotic replacement of Na^+ with hydrazinium (▲), methylammonium (■), and ethanolammonium (▼). (*B*) *I-V* relationship obtained in 140 mM Na^+, and after substitution of methylammonium, ethanolammonium and hydrazinium for Na^+. Symbols same as in *A*. The data points represent the mean peak current amplitude ± SEM for at least four cells.
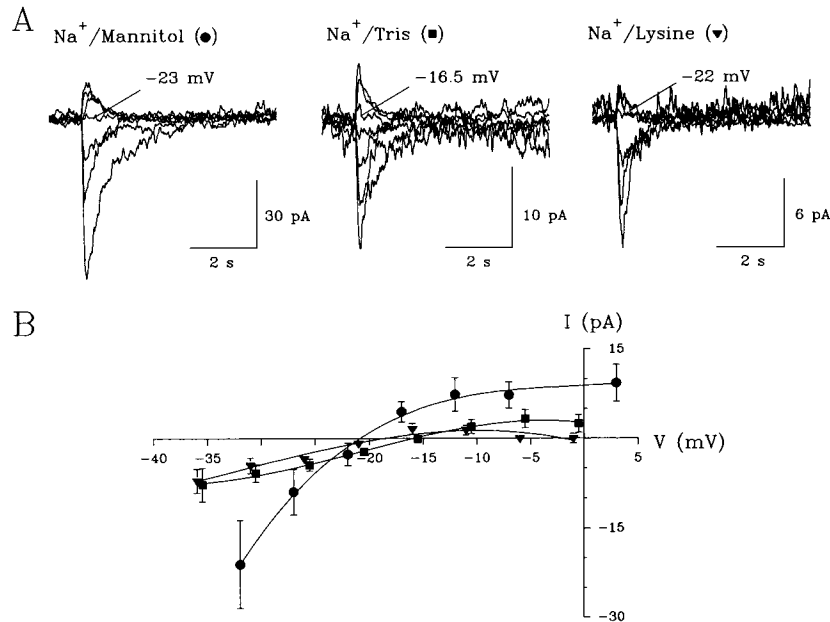
FIGURE 7. Reversal potential measurements of ACh-evoked currents obtained for mixtures of poorly permeant organic cations. (A) ACh-evoked currents recorded at 5-mV intervals after replacement of half of the external Na^+ concentration with 140 mM mannitol (●), 70 mM Tris (■) or 70 mM lysine (▼). (B) Peak I-V relations obtained for 50% Na^+ mixtures with mannitol, Tris and lysine. The interpolated reversal potential was −20.9 mV for the 50% Na^+/mannitol solution. Reversal potentials for 50% Na^+/Tris and 50% Na^+/lysine solutions are −15.8 mV and −19.8 mV, respectively. Symbols same as A. Points represent the mean peak current amplitude ± SEM of at least four cells.

Bis-Tris. The measured shifts in reversal potential and calculated relative permeabilities for isotonic solutions and Na^+ mixtures of permeant organic cations are presented in Table III. Permeability ratios ranged from 1.8 and 1.15 for the amino (hydrazine) and methyl (methylamine) derivatives of ammonium, to <0.01 for the

TABLE III

ΔE_r and Permeability Ratios For Organic Cations

X	ΔE_r ± SEM			P_X/P_{Na}
	Mol Wt	mV	n	
140 Na^+	23.0	0.0	—	1.00
140 Methylamine	32.1	+3.7 ± 0.7	5	1.15
140 Hydrazine (pH 6.6)	33.1	+16.1 ± 1.2	4	1.80
140 Ethanolamine	62.1	−5.8 ± 0.6	4	0.80
70 Na^+/140 Mannitol	182.2	−20.9 ± 0.9	10	—
70 Na^+/70 Tris	122.1	−15.8 ± 0.4	5	0.18
70 Na^+/70 Lysine	147.2	−19.8 ± 1.6	4	<0.01

Reference solution (in millimolar): 140 NaCl, 7.7 Glucose, 10 Histidine, pH 7.2. Internal solution (in millimolar): 130 NaCl, 2 Na_2ATP, 5 Na_4BAPTA, 10 HEPES, pH 7.2.
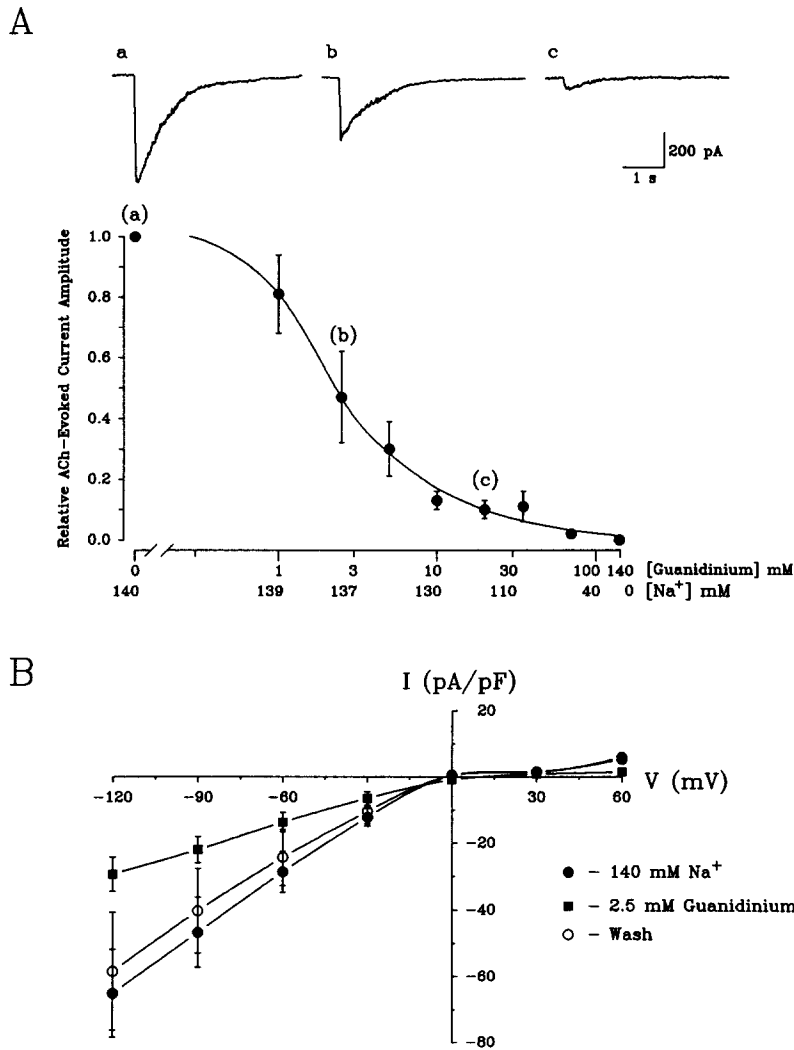
FIGURE 8.   Inhibition of ACh-evoked currents by external guanidinium ions. (A) Dependence of the relative whole-cell ACh–evoked current amplitude on external guanidinium mole fraction. ACh-evoked current amplitude was measured at a holding potential of -90 mV in an extracellular solution in which Na^+ was replaced by guanidinium. The curve is a best fit of the data by a single-site adsorption isotherm using Eq. 2 with a half-maximal inhibition (IC_{50}) of 2.5 mM. Each point represents the mean $\pm$ SEM for four cells. Representative ACh-induced currents obtained in the absence (a), and presence of 2.5 (b) and 20 mM (c) guanidinium are shown above. (B) Normalized I-V relationship of ACh-evoked currents obtained in 140 mM NaCl (●), after isoosmotic substitution of 2.5 mM guanidine.Cl for NaCl (■) and upon return to isotonic NaCl (○). Each point represents the mean $\pm$ SEM from three cells.

amino acid, lysine. The shift produced by 50% lysine ($\Delta E_{rev} = -19.9$ mV) is not statistically different from that obtained with a 50% Na^+ solution.

Block of ACh-evoked Currents by Organic Cations

Whereas significant ACh-evoked currents are carried by organic cations through the AChR channel at the frog motor endplate, no ACh-evoked currents were supported by the majority of organic cations tested in rat parasympathetic neurons. An example
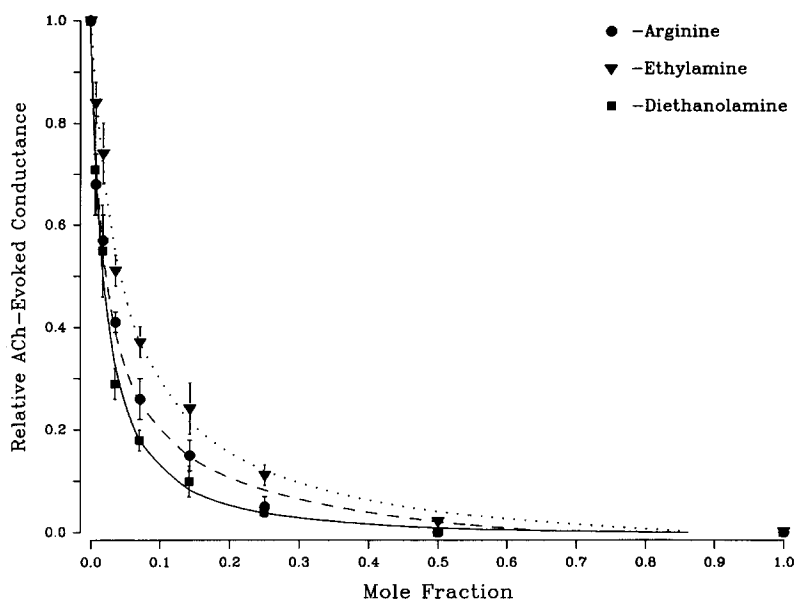

FIGURE 9. Inhibition of ACh-evoked currents by external organic cations. Mole fraction dependence of relative ACh-induced conductance determined from currents recorded after isotonic replacement of external Na^+ with increasing concentrations of ethylamine (▼), diethanolamine (■) or arginine (●). Relative ACh-evoked chord conductance at each concentration of test cation was calculated using a reversal potential estimated from the relative permeabilities for these organic cations obtained at the motor endplate AChR channel (Dwyer et al., 1980). The curves represent the best fit of the data by a single-site adsorption isotherm using Eq. 2, with IC_{50}'s of 6, 2.5, and 3.3 mM for ethylamine, diethanolamine and arginine, respectively. The data points represent the mean relative conductance ± SEM from a minimum of four cells.

of the relationship between ACh-evoked peak current amplitude and the $Na^+/$ guanidinium ratio of the external solution is plotted in Fig. 8 A. Isotonic replacement of NaCl by guanidine.Cl in the extracellular solution reduced ACh-evoked currents in a dose-dependent manner. The best fit of the data to a single-site adsorption isotherm gave an IC_{50} for inhibition of ACh-evoked currents by guanidinium of 2.5 mM. *I-V* relationships determined in the absence and presence of 2.5 mM guanidinium are plotted in Fig. 8 B ($n = 3$). The lack of voltage dependence of the guanidinium block of ACh-evoked currents could imply that the binding site for this

cation is located outside the membrane electric field, or more likely is an internal site equally accessible from both sides of the membrane.

Substitution of ethylamine, diethanolamine and arginine for Na^+ in the external solution inhibited ACh-activated currents in a manner similar to that observed for guanidinium. The relative ACh-evoked chord conductance at -90 mV plotted as a function of the mole fraction of external organic cation is shown in Fig. 9. The concentrations of the saturated compounds, ethylamine ($IC_{50} = 6.0$ mM) and diethanolamine ($IC_{50} = 2.5$ mM), required for half-maximal inhibition of ACh-evoked currents were similar to those determined for the unsaturated compounds, guanidine and arginine ($IC_{50} = 3.3$ mM). The molecular size of the test cation also appears to play little role in determining the effectiveness of block, as the mean ionic diameter of these cations, determined from space-filling Corey-Pauling-Koltum (CPK) models, ranged from 4.44 Å for guanidine to 6.96 Å for arginine. Although no ACh-evoked currents were observed for these organic cations at concentrations > 70 mM, inward ACh-evoked currents were obtained in the presence of ethanolamine and Tris as charge carriers, with mean diameters of 4.53 and 5.82 Å, respectively. Solutions of primary, secondary and tertiary amines have been shown to exhibit agonist action in cultured rat myotubes (Sanchez et al., 1986). Although the organic cations alone (in the absence of ACh) failed to evoke a change in the holding current per se, desensitization of the nicotinic ACh receptor by the organic cations tested may contribute to the observed inhibition of ACh-evoked currents in rat parasympathetic neurons.

DISCUSSION

The transient inward current elicited at negative membrane potentials in response to exogenously applied ACh in parasympathetic neurons of rat intracardiac ganglia is due to the activation of cation-selective nAChR channels which exhibit negligible anion permeability (Fieber and Adams, 1991). Neuronal nAChR channels in rat sympathetic ganglia (Trouslard et al., 1993), rat retinal ganglion cells (Lipton, Aizenman, and Loring, 1987) and rat medial habenular nucleus (Mulle and Changeux, 1990) are also cation selective. These and the present ionic selectivity studies use the measurement of shifts in the reversal potential upon ion substitution to calculate the relative permeability using the GHK voltage equation. There was no simple correlation between the shifts in reversal potential and magnitude of the whole-cell ACh-evoked currents observed with the monovalent inorganic cations. The peak amplitudes of ACh-evoked currents obtained in isotonic NH_4^+ or K^+ solutions were similar to that obtained in isotonic Na^+, whereas the current amplitudes were smaller in isotonic solutions of other alkali cations (see Fig. 2). The (E_{rev}) selectivity sequence of monovalent alkali metal cations for the neuronal nAChR channel of rat parasympathetic neurons, $Cs^+ > K^+ > Rb^+ > Na^+ > Li^+$, follows the free solution mobility ratios of the cations with the exception of Rb^+, which has a lower permeability than that expected for free diffusion of Rb^+ through the channel. This selectivity sequence corresponds to a variant of Eisenman sequence II, indicating that the narrow region of the ion conducting pore of the channel acts like a low field strength site (Eisenman, 1962). The weak selectivity of the neuronal nAChR channel to monovalent cations is evident also in the permeability ratios (P_x/P_{Na}), which

ranged from 1.27 (Cs^+) to 0.75 (Li^+). The selectivity sequence of the neuronal nAChR channel is similar to that obtained for the nAChR channel of the frog motor endplate (Adams et al., 1980) and of rat paratracheal ganglion cells (Aibara and Akaike, 1991): $Cs^+ > Rb^+ > K^+ > Na^+ > Li^+$. The ionic selectivity sequence of the nAChR channel in rat sympathetic neurons for alkali cations is $K^+ > Na^+ > Li^+ > Cs^+$ (Trouslard et al., 1993) which also differs from the single-channel conductance sequence: $K^+ > Cs^+ > Na^+ > Li^+$ (Mathie et al., 1991). The 5-hydroxytryptamine (5-HT$_3$) receptor channel, a nonselective cation channel, also distinguishes poorly among monovalent metal cations (Yang, 1990).

The neuronal nAChR channel also accepts the divalent alkaline earths, in the order $Mg^{2+} > Sr^{2+} > Ba^{2+} > Ca^{2+}$, with the GHK permeability ratios (P_x/P_{Na}) of 1.10, 0.78, 0.72, and 0.65, respectively. This is different from the selectivity sequence determined for the skeletal muscle nAChR channel where Mg^{2+} (0.18) $> Ca^{2+}$ (0.16) $> Ba^{2+}$ (0.13) $> Sr^{2+}$ (0.10) (Adams et al., 1980), and implies that the relative divalent cation permeability of the neuronal nAChR channel is ~ fivefold higher than that of the motor endplate channel (cf. Vernino, Rogers, Radcliffe, and Dani, 1994). The relative Ca^{2+} permeability of the nAChR channel in rat parasympathetic neurons is lower than that reported for nAChR channels in rat sympathetic neurons (P_{Ca}/P_{Na} = 3.8, Trouslard et al., 1993), PC12 cells (P_{Ca}/P_{Na} = 2.54, Sands and Barish, 1991) and bovine chromaffin cells (P_{Ca}/P_{Na} = 2.53, Nooney et al., 1992; P_{Ca}/P_{Cs} = 1.5, Vernino et al., 1992). However, the presence of ACh-evoked currents recorded in isotonic Ca^{2+} external solution indicate that there is a significant Ca^{2+} influx through the open nAChR channel (see Fig. 3 A). Indeed, the neuronal nAChR channel had a single-channel slope conductance of ~20 pS in isotonic Ca^{2+} (Adams and Nutter, 1992), compared to a value of 11 pS for the nAChR channel of rat medial habenula neurons (Mulle et al., 1992), 12 pS for the nAChR channel in clonal BC3H1 mouse muscle cells (Decker and Dani, 1990), or 14 pS reported for the N-methyl-D-aspartate (NMDA) receptor channel in cultured central neurons (Mayer and Westbrook, 1987).

In isotonic Mn^{2+}, inward and outward currents were clearly resolved; a relative permeability ratio of 0.67 was obtained for Mn^{2+}. No ACh-evoked currents, however, were detected with the transition metal cations Ni^{2+}, Zn^{2+}, or Cd^{2+} in either isotonic solutions or in 50% mixtures with Na^+. The strong block of ACh-induced currents by Ni^{2+}, Zn^{2+} and Cd^{2+} with IC_{50}'s of 500 μM, 5.2 μM and 1 mM, respectively, clearly distinguishes this neuronal from muscle nAChR channels. In the frog endplate, transition metal cations are permeant, yielding permeability ratios similar to those of Ca^{2+} and Mg^{2+} (P_x/P_{Na} = 0.13 − 0.26; Adams et al., 1980). The NMDA receptor channel of mouse central neurons has also been shown to be blocked by Ni^{2+}, Zn^{2+}, and Cd^{2+} (Mayer and Westbrook, 1985; Westbrook and Mayer, 1987), and required similar concentrations for half-maximal inhibition as those determined for the neuronal nAChR channel. The block of NMDA-activated conductances in mouse central neurons by Zn^{2+} appears to be due to an external binding site for Zn^{2+}, whereas the voltage dependence of Zn^{2+} block of ACh-evoked currents in rat parasympathetic neurons suggests that a binding site may be within the membrane electric field.

The effects of external pH on neuronal nAChR channels are similar to those

observed for nAChR channels at the frog motor endplate (Landau, Gavish, Nachshen, and Lotan, 1981). The current amplitude was maximal at pH 8.0 and became smaller with both more acidic or basic pH values. This inhibition was independent of the membrane potential, suggesting that the respective titratable charged groups are located outside the ion conducting pore. The nonmonotonic effect of external pH on current amplitude is unlikely to be due to the screening of membrane surface charges (see Hille, 1992).

Permeability ratios could be determined for only six of the seventeen organic cations examined. As with the inorganic cations, there was no simple correlation between the whole-cell ACh–evoked current amplitude and the permeability ratio determined from ΔE_{rev}. ACh-evoked current amplitudes obtained in isotonic hydrazinium or methylammonium solutions (permeability ratios of 1.8 and 1.15, respectively) were only 25–40% of the peak current amplitudes recorded in Na^+ solutions. Comparison of permeability ratios (Table III) with those determined for the nAChR channel of the motor endplate reveal a similarity which is found also with two other ligand-gated cation channels, the 5-HT₃ receptor of mouse neuroblastoma N18 cells (Yang, 1990) and the kainate receptor of chick central neurons (Vyklicky, Krusek, and Edwards, 1988). The relative permeability ratios determined for methylammonium, ethanolammonium, and Tris at the neuronal nAChR channel are, however, two- to sevenfold higher than the values obtained for the NMDA receptor channel of chick central neurons (Vyklicky et al., 1988).

In this study, we have examined permeation and block of inorganic and organic cations at the nicotinic AChR channel of parasympathetic neurons. The relatively high single-channel conductance (~30 pS in symmetric 140 mM NaCl; Adams and Nutter, 1992) and weak discrimination among the inorganic metal cations suggest that, like the motor endplate channel, the ion conducting pore of the neuronal nAChR channel acts as a water-filled pore containing no negative charges of high field strength. Given the small number of permeant organic cations, the influence of the structure of the organic cation (e.g., linear vs branched structure, saturated vs unsaturated) on ion permeation could not be assessed in detail. For those organic cations found to be measureably permeant, there is, however, a correlation between the size of the organic cation and the calculated permeability ratio. A plot of the relationship between the relative permeabilities and the molecular dimensions of permeant cations is shown in Fig. 10. The relative permeabilities of the organic cations (*filled symbols*) vary inversely with increasing mean diameter. Modeling the channel as a cylindrical pore and fitting the permeability data for organic cations (see Dwyer et al., 1980) yields a minimum pore diameter of 7.6 Å. Lysine was the only test cation approaching the theoretical diameter of the pore. This estimated pore diameter agrees closely with the diagonal of the pore determined for the nAChR channel of frog muscle (7.7 Å; Dwyer et al., 1980) and the cross-section of the nAChR channel of cat superior cervical ganglion neurons (6.1 × 8.3 Å; Zhorov, Brovtsyna, Gmiro, Lukomskaya, Serdyuk, Potapyeva, Magazanik, Kurenniy, and Skok, 1991). The pore dimensions are also similar to those proposed for the 5HT receptor channel (7.6-Å diam; Yang, 1990), and the kainate and NMDA receptor channels (6.5 Å and 6.0 Å diam, respectively; Vyklicky et al., 1988).

Our data indicate that the apparent pore geometries of the neuronal and muscle

nAChR channels are similar but the pore linings are likely different. Structural modeling of ion transport data suggests that the permeability and conductance properties of the muscle nAChR channel can be explained by a charged outer vestibule tapering to a single ion binding site within the narrow region of the ion-conducting pore (Dani and Eisenman, 1987). This view has been supported by studies utilizing site-directed mutagenesis of the muscle nAChR channel in combination with single-channel recording (Imoto et al., 1986; Imoto et al., 1988; Villarroel,
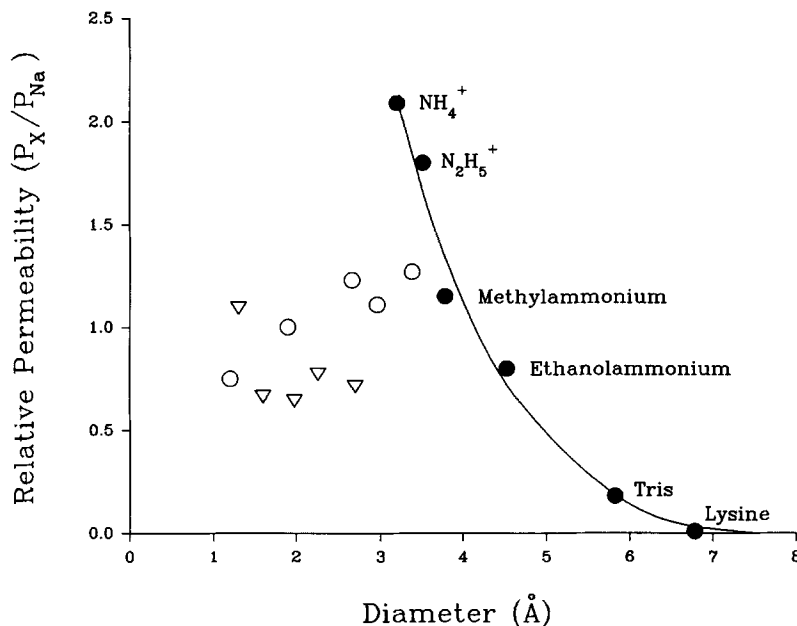

FIGURE 10. The relationship between relative permeability and mean ionic diameter for permeant cations. The geometric mean diameters (●) of organic cations were determined from space-filling CPK models, and monovalent metal (○) and alkaline earth (∇) ionic crystal diameters are from Pauling (1960). The curve represents the best fit of the data according to the equation

$$P_x/P_{Na} = \frac{20.3}{a}\left(1 - \frac{a}{b}\right)^2, \tag{2}$$

where a is the ionic diameter, P_x/P_{Na} is the relative permeability and b is the pore diameter of the channel. The open pore size determined from the fit is 7.6 Å.

Herlitze, Koenen, and Sakmann, 1991; Konno, Busch, von Kitzing, Imoto, Wang, Nakai, Mishina, Numa, and Sakmann, 1991; Cohen, Labarca, Czyzyk, Davidson, and Lester, 1992a; Cohen, Labarca, Davidson, and Lester, 1992b). The difference in the ion permeability properties between the nAChR channel of rat parasympathetic neurons and that of skeletal muscle may reflect differences in the primary structures of the channel proteins, and in particular, the M2 region and adjacent residues (see Fig. 5; Adams and Nutter, 1992). The present results provide constraints to possible

molecular structures of nAChR channels in mammalian parasympathetic neurons, and allow comparison to neuronal nAChR channels in other regions of the nervous system.

REFERENCES

Adams, D. J., T. M. Dwyer, and B. Hille. 1980. The permeability of endplate channels to monovalent and divalent metal cations. *Journal of General Physiology.* 75:493–510.

Adams, D. J., W. Nonner, T. M. Dwyer, and B. Hille. 1981. Block of endplate channels by permeant cations in frog skeletal muscles. *Journal of General Physiology.* 78:593–615.

Adams, D. J., and T. J. Nutter. 1992. Calcium permeability and modulation of nicotinic acetylcholine receptor-channels in rat parasympathetic neurons. *Journal de Physiologie.* 86:67–76.

Aibara, K., and N. Akaike. 1991. Acetylcholine-activated ionic currents in isolated paratracheal ganglion cells of the rat. *Brain Research.* 558:20–26.

Anand, R., W. G. Conroy, R. Schoepfer, P. Whiting, and J. Lindstrom. 1991. Neuronal nicotinic acetylcholine receptors expressed in *Xenopus* oocytes have a pentameric quaternary structure. *Journal of Biological Chemistry.* 266:11192–11198.

Butler, J. N. 1968. The thermodynamic activity of calcium ion in sodium chloride-calcium chloride electrolytes. *Biophysical Journal.* 8:1426–1432.

Cohen, B. N., C. Labarca, L. Czyzyk, N. Davidson, and H. A. Lester. 1992a. $Tris^+/Na^+$ permeability ratios of nicotinic acetylcholine receptors are reduced by mutations near the intracellular end of the M2 region. *Journal of General Physiology.* 99:545–572.

Cohen, B. N., C. Labarca, N. Davidson, and H. A. Lester. 1992b. Mutations in M2 alter the selectivity of the mouse nicotinic acetylcholine receptor for organic and alkali metal cations. *Journal of General Physiology.* 100:373–400.

Cooper, E., S. Couturier, and M. Ballivet. 1991. Pentameric structure and subunit stoichiometry of a neuronal nicotinic acetylcholine receptor. *Nature.* 350:235–238.

Dani, J. A., and G. Eisenman. 1987. Monovalent and divalent cation permeation in acetylcholine receptor channels. *Journal of General Physiology.* 89:959–983.

Decker, E. R., and J. A. Dani. 1990. Calcium permeability of the nicotinic acetylcholine receptor: the single-channel calcium influx is significant. *Journal of Neuroscience.* 10:3413–3420.

Dwyer, T. M., D. J. Adams, and B. Hille. 1980. The permeability of the endplate channel to organic cations in frog muscle. *Journal of General Physiology.* 75:469–492.

Eisenman, G. 1962. Cation selective glass electrodes and their mode of operation. *Biophysical Journal.* 2:259–323.

Fieber, L. A., and D. J. Adams. 1991. Acetylcholine-evoked currents in cultured neurones dissociated from rat parasympathetic cardiac ganglia. *Journal of Physiology.* 434:215–237.

Hamill, O. P., A. Marty, E. Neher, B. Sakmann, and F. J. Sigworth. 1981. Improved patch-clamp techniques for high-resolution current recording from cells and cell-free membrane patches. *Pflügers Archiv.* 391:85–100.

Hille, B. 1975. Ionic selectivity of Na and K channels of nerve membranes. *In* Membranes: A Series of Advances. Vol. 3. Dynamic Properties of Lipid Bilayers and Biological Membranes. G. Eisenman, editor. Marcel Dekker, Inc., New York. 255–323.

Hille, B. 1992. Modifiers of gating. *In* Ionic Channels of Excitable Membranes. Second edition. Sinauer Associates Inc., Sunderland, MA. 462–469.

Imoto, K., C. Busch, B. Sakmann, M. Mishina, T. Konno, J. Nakai, H. Bujo, Y. Mori, K. Fukuda, and S. Numa. 1988. Rings of negatively charged amino acids determine the acetylcholine receptor channel conductance. *Nature.* 335:645–648.

Imoto, K., C. Methfessel, B. Sakmann, M. Mishina, Y. Mori, T. Konno, K. Fukuda, M. Kurasaki, H. Bujo, Y. Fujita, and S. Numa. 1986. Location of a δ-subunit region determining ion transport through the acetylcholine receptor channel. *Nature.* 324:670–674.

Konno, T., C. Busch, E. von Kitzing, K. Imoto, F. Wang, J. Nakai, M. Mishina, S. Numa, and B. Sakmann. 1991. Rings of anionic amino acids as structural determinants of ion selectivity in the acetylcholine receptor channel. *Proceedings of the Royal Society of London B.* 244:69–79.

Landau, E. M., B. Gavish, D. A. Nachshen, and I. Lotan. 1981. pH dependence of the acetylcholine receptor channel. *Journal of General Physiology.* 77:647–666.

Leutje, C. W., and J. Patrick. 1991. Both α- and β-subunits contribute to the agonist sensitivity of neuronal nicotinic acetylcholine receptors. *Journal of Neuroscience.* 11:837–845.

Leutje, C. W., K. Wada, S. Rogers, S. N. Abramson, K. Tsuji, S. Heinemann, and J. Patrick. 1990. Neurotoxins distinguish between different neuronal nicotinic acetylcholine receptor subunit combinations. *Journal of Neurochemistry.* 55:632–640.

Lewis, C. A. 1979. Ion-concentration dependence of the reversal potential and the single channel conductance of ion channels at the frog neuromuscular junction. *Journal of Physiology.* 286:417–445.

Lewis, C. A. 1984. Divalent cation effects on acetylcholine-activated channels at the frog neuromuscular junction. *Cellular and Molecular Neurobiology.* 4:273–284.

Lipton, S. A., E. Aizenman, and R. H. Loring. 1987. Neural nicotinic acetylcholine responses in solitary mammalian retinal ganglion cells. *Pflügers Archiv.* 410:37–43.

Lukas, R. J., and M. Bencherif. 1992. Heterogeneity and regulation of nicotinic acetylcholine receptors. *International Review of Neurobiology.* 34:25–131.

Mathie, A., S. G. Cull-Candy, and D. Colquhoun. 1991. Conductance and kinetic properties of single nicotinic acetylcholine receptor channels in rat sympathetic neurones. *Journal of Physiology.* 439:717–750.

Mayer, M. L., and G. L. Westbrook. 1985. The action of N-methyl-D-aspartic acid on mouse spinal neurones in culture. *Journal of Physiology.* 361:65–90.

Mayer, M. L., and G. L. Westbrook. 1987. Permeation and block of N-methyl-D-aspartic acid receptor channels by divalent cations in mouse cultured central neurones. *Journal of Physiology.* 394:501–527.

Mulle, C., and J. P. Changeux. 1990. A novel type of nicotinic receptor in the rat central nervous system characterized by patch-clamp techniques. *Journal of Neuroscience.* 10:169–175.

Mulle, C., D. Choquet, H. Korn, and J. P. Changeux. 1992. Calcium influx through nicotinic receptor in rat central neurons: its relevance to cellular regulation. *Neuron.* 8:135–143.

Nooney, J. M., J. A. Peters, and J. J. Lambert. 1992. A patch clamp study of the nicotinic acetylcholine receptor of bovine adrenomedullary chromaffin cells in culture. *Journal of Physiology.* 455:503–527.

Nutter, T. J., and D. J. Adams. 1991. The permeability of neuronal nicotinic receptor-channels to monovalent and divalent inorganic cations. *Biophysical Journal.* 59:34a. (Abstr.)

Papke, R. L. 1993. The kinetic properties of neuronal nicotinic receptors: genetic basis of functional diversity. *Progress in Neurobiology.* 41:509–531.

Pauling, L. 1960. Table 13-3. *In* Nature of the Chemical Bond. Third edition. Cornell University Press, Ithaca, New York.

Robinson, R. A., and R. H. Stokes. 1965. *In* Electrolyte Solutions. Second edition. Butterworth and Co., Ltd., London. 479–496.

Sanchez, J. A., J. A. Dani, D. Siemen, and B. Hille. 1986. Slow permeation of organic cations in acetylcholine receptor channels. *Journal of General Physiology.* 87:985–1001.

Sands, S. B., and M. E. Barish. 1991. Calcium permeability of neuronal nicotinic acetylcholine receptor channels in PC12 cells. *Brain Research.* 560:38–42.

Sargent, P. B. 1993. The diversity of neuronal nicotinic acetylcholine receptors. *Annual Reviews in Neuroscience.* 16:403–443.

Trouslard, J., S. J. Marsh, and D. A. Brown. 1993. Calcium entry through nicotinic receptor channels and calcium channels in cultured rat superior cervical ganglion cells. *Journal of Physiology.* 468:53–71.

Vernino, S., M. Amador, C. W. Luetje, J. Patrick, and J. A. Dani. 1992. Calcium modulation and high calcium permeability of neuronal nicotinic acetylcholine receptors. *Neuron.* 8:127–134.

Vernino, S., M. Rogers, K. A. Radcliffe, and J. A. Dani. 1994. Quantitative measurement of calcium flux through muscle and neuronal nicotinic acetylcholine receptors. *The Journal of Neuroscience.* 14:5514–5524.

Villarroel, A., S. Herlitze, M. Koenen, and B. Sakmann. 1991. Location of a threonine residue in the α-subunit M2 transmembrane segment that determines the ion flow through the acetylcholine receptor channel. *Proceedings of the Royal Society of London B.* 213:69–74.

Vyklicky, L., J. Krusek, and C. Edwards. 1988. Differences in the pore sizes of the N-methyl-D-aspartate and kainate cation channels. *Neuroscience Letters.* 89:313–318.

Westbrook, G. L., and M. L. Mayer. 1987. Micromolar concentrations of Zn^{2+} antagonize NMDA and GABA responses of hippocampal neurons. *Nature.* 328:640–643.

Woodhull, A. M. 1973. Ionic blockage of sodium channels. *Journal of General Physiology.* 61:687–708.

Yang, J. 1990. Ion permeation through 5-hydroxytryptamine-gated channels in neuroblastoma N18 cells. *Journal of General Physiology.* 96:1177–1198.

Zhorov, B. S., N. B. Brovtsyna, V. E. Gmiro, N. Y. Lukomskaya, S. E. Serdyuk, N. N. Potapyeva, L. G. Magazanik, D. E. Kurenniy, and V. I. Skok. 1991. Dimensions of the ion channel in neuronal nicotinic acetylcholine receptor as estimated from analysis of conformation-activity relationships of open-channel blocking drugs. *Journal of Membrane Biology.* 121:119–132.